Biomaterials Science

Trifluoromethyl-Functionalized Poly(lactic acid): A Fluoropolyester Designed for Blood Contact Applications

Journal:	*Biomaterials Science*
Manuscript ID	BM-ART-03-2019-000353.R2
Article Type:	Paper
Date Submitted by the Author:	04-Jul-2019
Complete List of Authors:	Khalifehzadeh, Razieh; University of Washington, Chemical Engineering Ratner, Buddy; University of Washington, Department of Bioengineering

Trifluoromethyl-Functionalized Poly(lactic acid): A Fluoropolyester Designed for Blood Contact Applications

Razieh Khalifehzadeh[1], Buddy D. Ratner [*,1, 2]

[1]Department of Chemical Engineering, University of Washington, Seattle, USA
[2]Department of Bioengineering, University of Washington, Seattle, USA

*Corresponding author:

E-mail address: ratner@uw.edu

Keywords: Fluoropolymer, Hemocompatibility, Protein adsorption, Poly(lactic acid), Biomaterials, organic synthesis

Abstract

Fluorinated polymers are strong candidates for development of new cardiovascular medical devices, due to their lower thrombogenicity as compared to other polymers used for cardiovascular implants. Few studies have reported the development of fluorinated polyesters and their potential in blood contact applications has never been examined. In this study, we developed a versatile method for preparing trifluoromethyl-functionalized poly(lactic acid) that can be potentially extended to prepare a new class of polyesters with various halogen or halocarbon substitutions. The resulting fluorinated polymer was hydrophobic relative to poly(lactic acid) and extracts from this polymer showed no *in vitro* cytotoxicity to NIH-3T3 mouse fibroblast cells. A preliminary consideration of the blood interactions of the CF_3-functionalized polyester was evaluated by measuring the amount of the adsorbed albumin and fibrinogen from human blood plasma. The fluorinated polyester adsorbed and retained higher amounts of albumin and fibrinogen with a higher albumin/fibrinogen ratio as compared to poly(lactic acid), suggesting enhanced hemocompatibility. Plasma protein

adsorption is the first event that occurs seconds after device implantation and controlling the adsorbed proteins will dictate the performance of medical implants.

1. Introduction

Polyesters derived from lactic/glycolic acid are widely used in various biomedical applications such as drug delivery, sutures and implants [1-4]. Attempts have been made to expand the application spectrum of these polymers by modifying their inherent physiochemical properties. Typical strategies include copolymerization and block copolymer preparation [5]. Alternatively, modifications may be introduced using well-designed lactic/glycolic acid derivatives as monomers for preparing polylactides/glycolides [6, 7]. Various functional groups including alkyl, allyl, hydroxyl, carboxylic acid , amine, polyethylene glycol (PEG) and alkenyl have been reported [8-13]. However, halogen-substituted lactides and particularly fluorine-substituted lactides, have

only infrequently been reported in the literature [14, 15]. The introduction of fluorine and fluorine-containing substituents impacts the properties of an organic compound. Fluorine is the most electronegative element and its size, hydrophobicity and electronic polarization can significantly affect chemical outcomes. For example, the trifluoromethyl (CF_3) group serves as an important component of many active pharmaceutical drugs [16-20]. Fluorinated polymers have been used in blood contacting applications such as vascular grafts, bypass grafts and in vivo oxygen transport (blood substitutes) and have been found by many researchers to reduce platelet adhesion and activation comparted to controls [21-23]. Using fluoropolymers such as polytetrafluoroethylene (PTFE) in orthopedic applications had poor outcomes due to the release of submicron wear particles.

We hypothesize that poly(lactic acid) modified to replace the methyl group with a trifluoro methyl group will demonstrate improved blood compatibility via its ability to preferentially adsorb the inert protein albumin, and to retain that albumin in competition with other proteins in plasma. It has been shown that a preadsorbed layer of Alb prevents subsequent adhesion of fibrinogen and reduces *in vitro* platelet adhesion producing a potentially less thrombogenic surfaces [24]. A poly(lactic acid) that was surface-derivatized with -CF_3 groups has been synthesized [25] and shows the ability to adsorb higher levels of

albumin and for that albumin layer to resist displacement. This study describes the synthesis and characterization of trifluoromethyl-functionalized poly(lactic acid) with CF_3- groups homogeneously distributed throughout the polymer. Our strategy involves substitution of the hydrogen or methyl group of the lactide repeat unit with a trifluoromethyl functional group. Applying the established polymerization method of ring-opening polymerization (ROP) generated CF_3-functionalized poly(lactic acid). The structure of the substituted polymer backbone remains unchanged and, due to its analogy to polylactide, such substituted polymers could basically be hydrolytically degradable. The hydrolysis of ester group in PLA backbone is the major degradation mechanism and it is driven by nucleophilic attack of hydroxide ions on carbonyl carbon [26, 27]. The following factors should be taken into consideration when predicting the degradation rate of the functionalized polymer. First, the electron withdrawing effect of fluorine, which makes the carbonyl group more electrophilic and susceptible to nucleophilic attack. Second, lack of crystallinity in the fluorinated polymer which accelerates the degradation and finally hydrophobicity which limits the access of water molecules to the ester groups in the polymer backbone and slows down the degradation. This paper describes enhancements in synthesis to that used by Lee *et al.* [15] and expands upon the physical and biological characterization of the CF_3-functionalized poly(lactic acid).

Substituted lactides have been known for over four decades with the synthesis of alkyl-substituted lactide originally reported by Schöllkopf *et al.* in 1979 [28] using the route outlined in Figure 1(A). The method involves step-by-step condensation, starting from an α-hydroxyl acid and an α-haloacyl halide. This synthesis method has proven to be versatile and was reported previously for preparing various alkyl and benzyl substituted lactides [8-10, 29].

2. Experimental Section

2.1. Materials

3,3,3-trifluorolactic acid (TFLA) and 2-bromopropionyl bromide (2-BPB) were purchased from Matrix Scientific (Columbia, USA) and Sigma-Aldrich, respectively and were used as received. Tin (II) 2-ethylhexanoate ($Sn(Oct)_2$) and benzyl alcohol were purchased from Sigma-Aldrich and purified by distillation prior to use. Acetonitrile (MeCN), dichloromethane (DCM) and triethylamine (NEt_3) was obtained from a Glass Contour solvent purification system. All other reagents and solvents were used as received from commercial sources. ^{1}H, ^{13}C and ^{19}F NMR analyses were carried out at room temperature in deuterated solvents (deuterated acetonitrile for monomer and deuterated chloroform for the polymer) on a Bruker AV700 or DRX499 MHz spectrometer. Chemical shifts are expressed in parts per million (ppm) downfield from tetramethylsilane with the residual protio-solvent used as chemical shift standard. ($CDCl_3$, ^{1}H: 7.26 ppm

and ^{13}C: 77.16 ppm; CD_3CN, ^{1}H: 1.94 ppm and ^{13}C: 1.39 and 118.69 ppm). Hexafluorobenzene (-164.9 ppm) was used as an internal standard for recording ^{19}F-NMR spectra.

2.2. Buffer solutions

The protein radiolabeling buffer used in this study is referred to as cPBSz and contained 0.01 M sodium phosphate, 0.01 M sodium citrate, 0.12 M sodium chloride, and 0.02 % sodium azide. Protein adsorption washing buffer is referred to as cPBSzI and contained all the components of cPBSz and 10 mM NaI. All salts were reagent grade and purchased from Sigma-Aldrich (St. Louis, MO) and used without further purification. Sodium dodecyl sulfate (SDS) (electrophoresis purity) was obtained from BioRad (Richmond, CA). A solution of 2% SDS was used to elute the adsorbed proteins. All the buffers were at pH 7.4.

2.3. Synthesis of CF_3-functionalized lactide monomer

Figure 1(B) shows the synthetic route for preparing trifluoromethyl-functionalized lactide monomer. Under argon gas flow, 3,3,3-trifluorolactic acid (43 mmol) was dissolved in 100 ml dry acetonitrile in a flame-dried three-neck flask. The mixture was placed in an ice bath and dry triethylamine (56 mmol) was added to the reaction flask. Then an equimolar amount of 2-

bromopropionyl bromide (54 mmol) was mixed in in 10 mL of dry acetonitrile and was added dropwise via syringe to the reaction flask. After the addition was complete, the ice bath was removed and the mixture was stirred at room temperature for 5 h. The resulting white precipitate was filtered off through Celite, and the filtrate was concentrated under reduced pressure. The resulting product was then dissolved in ethyl acetate and filtered again through Celite to remove any remaining salts. The removal of the ethyl acetate by rotary evaporation gave product (2b) as a brown oil.

To prepare the product (3), dry acetonitrile (700 ml) was added to a flame-dried three-neck flask under argon gas flow and placed in an ice bath. Next, sodium hydride (64.5 mmol) was added to the flask and stirred for 20 minutes. The product (2b) was dissolved in dry acetonitrile (100 ml) and was added dropwise to the flask using an addition funnel over 45 minutes. The ice bath was removed and the reaction mixture was stirred until it reached room temperature. The reaction flask was then transferred to an oil bath and stirred overnight at 75 °C under argon gas flow. At the end of the reaction time, the oil bath was removed and the resulting mixture was cooled to room temperature. The reaction mixture was filtered through Celite to remove the white precipitate and the acetonitrile was removed by rotary evaporation. The crude product was purified by silica gel flash column chromatography using dry premium grade silica gel and an ethyl

acetate: hexane mixture (1:2) as an eluent. The solvents were distilled off and the product was recrystallized from hexane/dichloromethane to give product (3) as a white powder. The polymer was composed of (*R,S)* (87.5 %) and (*R,R*) and (*S,S*) (12.5 %) stereorepeating units (31% yield).

2.4. Solution polymerization of CF_3-functionalized lactide monomer

Figure 1(C) shows the solution polymerization of monomer (3) in dry toluene at 110 °C. A reaction flask containing stir bar was fitted with septum, flame dried under vacuum, and charged with monomer (3) (1mmol) and filled with dry toluene (4 ml). Benzyl alcohol (0.01 mmol) and tin (II) 2-ethylhexanoate $Sn(Oct)_2$ (0.01 mmol) were added to the flask and used as an initiator and catalyst respectively. Prior to polymerization, the stock solution of benzyl alcohol and catalyst was prepared in dry benzene (0.1M). The flask was placed in an oil bath and heated for 20 h at 110 °C. The resulting mixture was cooled to room temperature and dried in a rotary evaporator and then dissolved in chloroform. The precipitate was filtered and chloroform was removed by rotary evaporator. The polymer was further dissolved in methanol, filtered and concentrated in the rotary evaporator. The resulting product was dissolved again in chloroform and precipitated in an ample amount of hexane. Next, hexane was removed by rotary evaporator to give a trifluoromethyl-functionalized poly(lactic acid) as a white

powder (76% yield). Polymerization conversion, degree of polymerization (DP) and molecular weights of the polymer were determined by ^{1}H NMR analysis.

2.5. Sample preparation for surface analysis and protein adsorption studies

Glass cover slips (8mm and 15mm, ProSci Corp) were used to prepare samples for surface analysis, water contact angle measurements and protein adsorption studies. These cover slips were mounted in a custom-fabricated holder, and cleaned in a 1/64 dilution of Isopanasol in Milli-Q water (C.R. Callen Corp, Seattle, WA) with ultrasonication for 20 min. They were then washed with Milli-Q water in three changes of wash liquid (15 minute ultrasonications). The cover slips were air dried and stored in a desiccator. Next, both sides of the coverslips were spin-coated with an ethyl methacrylate-methacryoxysilane copolymer (EMA-silane) (2.5% w/v) and baked at 60 °C overnight. Coverslips were then immersed in ethyl acetate twice for 1 h and once for 5 min. The ethyl acetate was replaced with fresh ethyl acetate after each cycle and the EMA-silane coated coverslips were air dried and stored in desiccator. This pretreatment technique has been shown to inhibit delamination of polymer coatings on coverslips.

Polymer solutions (2.5% w/v) in chloroform were prepared and both sides of the EMA-silane coated coverslips were spin-coated at 4000 rpm for 20 seconds and air dried and stored in desiccator until ready to use. For protein adsorption

studies, 316 stainless steel sheets (316 SS) were cut into 7x7 mm coupon and cleaned by ultrasonicating them in hexane, methylene chloride, acetone and methanol for 15 min for each solvent and then air drying and storing in a desiccator. For cytotoxicity studies, samples were soaked in 70% ethanol for 2h and then washed with sterile PBS for 20 min.

2.6. Surface analysis of CF_3-functionalized poly(lactic acid)

The chemical composition of CF_3-poly(lactic acid) samples was determined by electron spectroscopy for chemical analysis (ESCA) at the National ESCA and Surface Analysis Center for Biomedical Problems (NESAC/BIO, University of Washington, Seattle). A thin layer of the CF_3-poly(lactic acid) was coated on coverslips using the spin-coating technique as described above. Samples were presoaked in water for 1 h before ESCA analysis and then air-dried. Spectra were collected using a Surface Science SSX-100 spectrometer (Surface Science Instrument, Mountain View, CA) equipped with a monochromatic Al K_α x-ray source. The samples were analyzed at a 55° take-off angle probing the topmost 50-80 Å of the surface. Compositional survey scans (0-1000 eV) and high-resolution C1s scans were acquired at an analyzer pass energy of 150 eV with an x-ray spot size of approximately 1000 μm. High-resolution scans were then obtained at a pass energy of 50 eV and resolved into individual Gaussian peaks using a least-squares algorithm in the Service Physics SSI software. Peaks were

identified and integrated to calculate the atomic percentage using the peak areas under the elemental curves and linear background function. Each peak was referenced to the C (1s) hydrocarbon peak at 285 eV to account for the surface charge induced binding energy shift.

2.7. Contact angle goniometry

A Rame-Hart contact angle goniometer was used to measure the advancing contact angles by the sessile drop method. The instrument was equipped with CAM 200 software and ultrapure water was used as a probing liquid. Polymer coated coverslips (15 mm, as described earlier) were placed on top of the sample stage and four droplets were added to obtain the advancing contact angle curve. Three samples were measured for each group.

2.8. Cell culture

Mouse embryonic fibroblast cells (NIH-3T3) were purchased from the American Type Culture Collection (ATCC, Manassas, VA, USA). Cells were cultured in Dulbecco's Modified Eagle's Medium (DMEM), supplemented with 10% fetal bovine serum (FBS) and maintained according to the ATCC recommended protocol.

2.9. *In vitro* cytotoxicity evaluation

The cytotoxicity of the samples was evaluated using an elution method following the guidelines described in [International standard ISO 10993-5:2009(E): Biological evaluation of medical devices—Part 5: Tests for *in vitro* cytotoxicity]. This method specifies the incubation of cultured cells in contact with extracts of a material. Briefly, NIH-3T3 cells were seeded in 24-well plate ($1x10^4$ cells/well) and incubated in 0.5 ml DMEM culture media at 37 °C. At the same time, samples were placed for extraction into the wells of 24-well plate. We added 0.5 ml DMEM culture medium supplemented with 10% FBS into each well and incubated at 37 °C in a humidified atmosphere containing 5% CO_2. At 24 h, the media in the cell plates was removed and replaced with 0.5 ml of samples eluents. Extracts from tissue culture polystyrene (TCPS) was used as the negative control and extracts from latex was used as the positive control. Tissue culture polystyrene (TCPS) was used as the negative control and extracts from latex were used as the positive controls. Cell viability was evaluated using the 3-(4,5-dimethylthiazol-2-yl)-2,5-diphenyltetrazolium bromide (MTT) colorimetric method. NIH-3T3 cells were seeded into the 24-well tissue culture plate at an initial density of 50,000 cells/well and incubated overnight. The cell culture medium was then removed and replaced with the same amount of the extracting medium from samples. The metabolic activity of the cells was measured after 24 h incubation by addition of 50 μl of MTT (5 mg/ml) to each well. The cells were

incubated for an additional 2.5 h. Then MTT solution was removed and 0.5 ml dimethyl sulfoxide was added to each well and incubated for 30 min. A 200 μl of sample cocktail from each well was transferred into a 96-well plate and measured at 570 nm using a microplate reader (tunable VERSAmax microplate reader, Molecular Devices; Sunnyvale, CA).

2.10. Live/dead assay

We used a live/dead cell staining assay kit (Molecular Probes, Inc) to evaluate the cell viability of the sample groups at different time points. NIH-3T3 cells were seeded in 24-well plates at density 10,000 cells/well and incubated overnight. The culture media was then removed and cells were incubated with the sample extracts as described before. At the end of each designated time point, culture media was removed and cells were prepared for microscopy following the manufacturer's procedure. Briefly, cells were washed with PBS and incubated for 20 min with 200 μl of a staining solution containing of 4 μM calcein AM and 2 μM ethidium homodimer (EthD-1). The staining solution was then replaced with phenol red-free DMEM. Cell attachment and morphology were examined on a Nikon TE200 inverted microscope using rhodamine and FITC filters to visualize calcein AM-stained (live) and EthD-1-stained (dead) cells respectively. ImageJ software was used to analyze the images which were acquired in pseudocolored, greyscale.

2.11. Protein radiolabeling

Human albumin (Alb, Sigma, St. Louis, MO) and human fibrinogen (Fg, Enzyme Research, South Bend, IN) were radiolabeled with $Na^{125}I$ iodide (Perkin Elmer, Waltham, MA) using the iodine monochloride (ICl) method as previously described [25]. Briefly, radioactive $Na^{125}I$ was mixed with nonradioactive ICl and incubated on ice for 20 mins. The radioactive ^{125}ICl (ICl*) was formed by rapid iodide-iodine exchange. To achieve an appropriate degree of substitution a 2:1 ICl* to protein molar ratio was used for labeling Alb and 3:1 ICl*/protein molar ratio was used for labeling Fg. The unbound ^{125}I was separated from the radiolabeled protein by passing the reaction mixture through a disposable size-exclusion chromatography column (#732-2010 EconoPac 10DG, BioRad, Hercules, CA). The radiolabeled Alb and Fg were stored at -80°C and used within two weeks.

2.12. Protein adsorption and retention

A standard protein concentration (0.3 mg/ml for Alb and 0.03 mg/ml for Fg) equivalent to 1% human plasma concentration was used for each individual protein adsorption experiment. A study by Brash *et al*. [30] shows that fibrinogen adsorption onto the surface of different polymeric samples was highest at 1% plasma concentration. Influenced by these previous findings, we used the more stringent condition (1% plasma concentration) for testing the extent of Fg

adsorption to these surfaces. We should point out that for *in vivo* studies the plasma is not diluted and this factor should be taken into consideration when interpreting the future *in vivo* results. Human blood was collected from healthy donors by trained phlebotomists at the University of Washington Medical Center, under a protocol approved by the UW Human Subjects Institutional Review Board. All experiments were performed in accordance of University of Washington Human Subjects Division and experiments were approved by the ethics committee (UW HSD Internal Review Board) at the University of Washington, Seattle, WA. Informed consents were obtained from human participants in this study. Blood was drawn by venipuncture into vacutainers containing ACD anticoagulant (1:9 v/v) and then centrifuged at 180 g for 20 minutes at room temperature to obtain the plasma layer. Samples were first placed into 1.5 ml polystyrene cups and equilibrated by submersion in 0.75 ml of degassed cPBSzI for one hour at room temperature. Shortly before use, 2x concentration stock protein solutions (0.6 mg/ml Alb or 0.06 mg/ml Fg) and 2% citrated pooled plasma solutions were made and appropriate amounts of radiolabeled protein were added to the unlabeled protein solution to achieve a minimum of a 2:1 signal-to-noise ratio (~50 cpm/ng). This addition did not change the initial protein concentration since only a small quantity of radiolabeled protein was added to the unlabeled protein solution due to the high specific activity of ^{125}I-labeled protein. Protein adsorption experiments were initiated by adding 0.75 ml of the 2x concentration stock solution to the samples soaking in cPBSzI. The final

protein concentrations were consistent with 1% human plasma solution. Sample were then transferred to water bath at 37°C and incubated for 2 h. At the end of adsorption time, samples were washed three times with cPBSzI buffer and the radioactivity was measured with the Cobra II gamma counter (Packard Instruments). Protein retention was measured by incubating samples with 1 ml of 2% sodium dodecyl sulfate (SDS). After 24 h samples were rinsed three times with cPBSzI and transferred into new gamma counter tubes for measuring the radioactivity of the retained proteins.

2.13. Statistical Analysis

All statistical analyses were performed using GraphPad Prism 7 for MacOSX (GraphPad Software, La Jolla California USA). Significant differences amongst sample groups were evaluated by one-way analysis of variance (ANOVA) applying Dunnett's multiple comparisons test. Statistical significance assumed for $p < 0.05$, unless otherwise noted.

3. Results and Discussion:

3.1. CF_3-functionalized lactide monomer synthesis

Inspired by Schollkopf's original method, we further extended possible substitutions to include halogens or halocarbons (Figure 1(D)). To explore one of the possibilities of this synthetic method, we chose commercially available 3,3,3-

trifluorolactic acid as a starting precursor due to the relevance of the CF_3 functional group to biological applications. Previous studies on substituted lactides consisted of hydrocarbon chains in various lengths – the fluorocarbon substituent has never been described before. CF_3-functionalized lactide was prepared by an analogue of the reaction described by Schöllkopf *et al*. However, applying the exact reaction conditions described earlier did not yield stable CF_3-functionalized lactide. Fluorine is the most electronegative element in the periodic table and it can potentially add further challenges to the reaction progress by the inductive effect limiting reagents from participating in the desired reaction. To overcome this challenge, we modified the synthesis method as shown in Figure 1(B). 3. First, 3,3,3-trifluorolactic acid (1) was reacted with 2-bromopropionyl bromide to form an intermediate anhydride (2a), followed by intramolecular acyl-transfer giving a carboxylic acid intermediate (2b). Then, under basic conditions, the carboxylate intermediate (2c), derived from (2b), undergoes nucleophilic substitution to yield the desired cyclic lactide monomer (3). Each separate addition of the bases, NEt_3 in first step and NaH in second step, was considered to act as an HBr scavenger and also contribute to the formation of carboxylates. The original method using a one-portion addition of NEt_3 did not produce a desired yield probably due to the presence of the CF_3 group on the asymmetric center. Formation of (2b) directly from (1) might also be

considered. However, in the presence of NEt_3 we speculate that this reaction does not dominate because the reactivity of secondary hydroxy group of (1) is lower than the carboxylate anion [31] .

The progress of the reaction, formation of intermediate ester (2b) along with consumption of TFLA, was monitored by thin layer chromatography (ethyl acetate: hexane 1:2 eluent mixture, R_f: 0.65). The formation of the cyclic monomer (3), *i.e.*, ring closure, imposed additional challenges probably due to the hydrolysis of final product. Various modifications were tried [12, 31] but the best yield was obtained using dry acetonitrile and sodium hydride (NaH). The use of NaH as a strong non-nucleophilic base instead of NEt_3 resulted in a higher yield. Subtle variations in the reaction conditions including type and separate addition of the base in each step of the reaction sequence, solvent and temperature significantly affected the synthesis outcome compared to Schöllkopf's original method. The schematic of the reaction setup is shown in Figure S1.

^{1}H-NMR and ^{13}C-NMR (700 MHz, acetonitrile-d_3) spectrum of CF_3-functionalized lactide monomer are shown in Figures 2. The ^{1}H-NMR spectrum shows characteristic peaks related to the cyclized monomer. The methyl and methine (methylylidine) protons can be identified as a doublet near δ: 1.6 and a quartet near δ: 5.2. A quartet near δ: 5.7 is associated with the CF_3 group in the functionalized lactide and clearly shows the formation of CF_3-functionalized

lactide monomer. The polymer was composed of (*R,S)* (87.5 %) and (*R,R*) and (*S,S*) (12.5 %) stereorepeating units (31% yield). Analysis of the mixture by ^{1}H-NMR (Figure 2a) showed a doublet from the methyl protons of the (*R,S*) isomer with the coupling constant of J_{HH} = 6.8 Hz, while the methyl protons from the (*S,S*) and (*R,R*) isomers have a coupling constant of J_{HH} = 7.1 Hz. The smaller coupling constant from the protons of (*R,S*) stereoisomers relative to that of the (*S,S*) or (*R.R*) ones was also reported in a previous study by Nagase *et al*. [31]. The molecular structure of the functionalized monomer was confirmed by ^{1}H-NMR, ^{13}C-NMR and ^{19}F-NMR spectroscopy. ^{1}H-NMR spectroscopy (Figure 2a) showed that the methine protons next to the CF_3 groups of the (*R,S*) isomers are de-shielded due to the electron withdrawing CF_3 groups (δ: 5.7 ppm) compared to the methine protons next to the methyl groups at (δ: 5.25 ppm). In addition, the coupling constant of the quartet from the methine protons next to CF_3 groups (J_{HF} = 6.4 Hz) is different from the coupling constant of the quartet next to the methyl groups (J_{HH} = 6.8 Hz). Also, the equal integration from these methine groups is in agreement with the structure of the CF_3-functionalized lactide monomers. The structure of the functionalized monomer was further confirmed by ^{13}C-NMR. Carbon- fluorine couplings resulted from carbons of the CF_3 groups can be identified as a quartet (d) at δ: 120 ppm. Two singlets at δ: 14.4 ppm and 72.58 ppm were assigned to carbons of CH_3 (a) and CH (c) groups. Another

quartet (b) at δ: 72 ppm was ascribed to the carbon next to the CF_3 group in the monomer structure. In addition, 2D-NMR and ^{19}F-NMR (Figure S2) further confirmed the structure of the monomer. The sharp singlet at around –74.91 ppm in ^{19}F-NMR (^{1}H-decoupled, top spectra) was assigned to the CF_3 group in functionalized monomer. Further analysis without ^{1}H-decoupling (Figure S2(c)) shows the presence of diastereomers in the monomer. The splitting is about 8 Hz and is consistent for a three bond J_{FH} coupling.

3.2. Ring-opening polymerization

Generally, two methods have been used to prepare polylactide: (i) ring-opening polymerization of cyclic diesters or (ii) direct polycondensation of α-hydroxycarboxylic acids [32, 33]. Typically, direct polycondensation of lactide generates low molecular weight polymer whereas, ROP yield polymers with different terminal groups, and higher molecular weight [34, 35]. The monomer-to-initiator ratio also affects the molecular weight of the resulting polymer. Both water and alcohols can be used as initiators. Therefore, to achieve high molecular weight, water should be removed from all synthesis precursors and the reactant system [35]. This is considered to be challenging since water is the byproduct of polycondensation which favors depolymerization and eventually leads to low

molecular weight polymer [36]. Therefore, controlled ROP in the presence of metal catalysts is the preferred method to obtain high molecular weight polymer. Tin(II) 2-ethylhexanoate $Sn(Oct)_2$ is the most commonly used catalyst for the preparation of polylactides for medical applications [37, 38]. This catalyst not only is highly effective for polymerization but it is also recognized by Food and Drug Administration (FDA).

The bulk polymerization of lactide using $Sn(Oct)_2$ in the presence of water or alcohol as initiator at relatively high temperature (110-220 ºC) is the classical method for preparing poly(lactic acid). Figure 1(C) shows the ROP of CF_3-functionalized lactide monomer at 110 °C using $Sn(Oct)_2$ and benzyl (BnOH) alcohol as the initiator alcohol due to (i) its low volatility in the chosen temperature range, (ii) the benzyl ^{1}H-NMR signal at δ 7.4 ppm can be used to estimate the conversion and degree of polymerization and (iii) by removing the benzyl protecting group with H_2/Pd, the resulting polymer would be suitable for further functionalization with the reactive carboxylic acid end group [9].

Figure 3(a) shows the ^{1}H-NMR spectra of the CF_3-functionalized poly(lactic acid). Replacing the methyl group of lactide with a trifluoromethyl group did not significantly affect the polymerization rate of functionalized monomer. The molecular weights of the substituted polymers were determined by end group analysis using ^{1}H-NMR (Figure 3a). Number average molecular weights (Mn,

$_{NMR}$) was calculated by comparing the integration of peaks from the methyl groups (δ = 1.45 to 1.69 ppm) and methine groups (δ = 5.45 to 5.68 ppm) against those peaks assigned to the benzyl end groups (δ = 7.31 to 7.33 ppm). The molecular weights of the prepared polymers were found to range from 18-20 KDa. The signals from both multiple angle light scattering (MALS) and differential refractive index (DRI) detectors in gel permeation chromatography (GPC) using THF as an eluent were too weak to obtain the molecular weight of the polymer. In addition, the ^{19}F-NMR spectra of the CF_3-functionalized polymer are shown in Figure 3(b). We observed peak broadening in the polymer spectrum, which indicates a distribution of polymer chains with various molecular weights.

3.3. ESCA analysis

The ESCA wide scan spectrum of the CF_3-functionalized poly(lactic acid) is shown in Figure 4 (top). In addition to C1s and O1s peaks, an F1s peak is also present in the spectrum and no additional elements were detected. A C1s high resolution ESCA spectrum of CF_3-functionalized poly(lactic acid) is also presented in Figure 4 (bottom). After resolution of the spectra into individual Gaussian peaks, we can see that both spectral envelops are comprised of four primary C peaks: (1) a 285.0 eV peak corresponding to carbon with three bonds to hydrogen CH_3, (hydrocarbons), (2) a 288.2 eV peak corresponding to carbon

singly bonded to oxygen (C-O), (3) a 289.9 eV peak corresponding to carbons with three bonds to oxygens (O=C–O) and a 293.5 eV peak corresponding to C-F_3. The surface chemical compositions of PLA and PLA-F have also been calculated. The PLA films have about 62% of carbon and 38% of oxygen, a C/O ratio of 1.6 (O/C ratio of 0.6) with no other detectable elements. Whereas, PLA-F has 51.3 % of carbon, 28.9 % of oxygen and about 19.8% of fluorine with C/O ratio of 1.8.

3.4. Contact angles

Contact angle is a pseudo-thermodynamic parameter, which has been commonly used to estimate the hydrophobicity of a solid surface. Higher water contact angles in air reflect higher hydrophobicity and lower surface energy. We used the sessile drop technique to measure the contact angle of CF_3-functionalized poly(lactic acid). The resulting water static contact angles are shown in Figure 5 and were compared to the contact angle of water on a smooth polytetrafluoroethylene (PTFE) sheet. We observed significant differences in contact angles between CF_3-functionalized poly(lactic acid) as compared with other samples studied here. As expected smooth PTFE sheet has the highest contact angle: 102±1.8°, suggesting high hydrophobicity. The contact angle of the CF_3-functionalized poly(lactic acid) was to 88.21±1.5º as compared to PLA (contact angle: 70±1.3º). This increase in the contact angle of the CF_3-

functionalized poly(lactic acid) was expected with the introduction of the fluorine in PLA-F structure. Previous studies with perfluoro compounds also reported reduced surface energy [39-41]. The presence of the trifluoromethyl groups explains these observations [42, 43].

3.5. *In vitro* assessments of cytotoxicity

To evaluate the cytotoxicity of the CF_3-functionalized poly(lactic acid) and to determine if harmful components are leaching from the polymer, conditioned medium was prepared by incubating samples in cell culture media according to ISO 10993-5. Then NIH-3T3 fibroblast cells were incubated with these material extracts. At the end of designated times, the media was removed and cytotoxicity of samples was evaluated by comparing with metabolic activity of cells treated with latex as a positive control using an MTT assay. MTT is a yellow tetrazolium salt that is reduced to form violet formazan crystals only in metabolically active cell mitochondria allowing us to quantify the number of living cells spectrophotometrically. The results were normalized with respect to the negative controls (TCPS) (Figure S3). There was no adverse effect on the metabolic activity of fibroblast cells treated with sample extracts and their MTT level was always above the 70% toxicity limit defined by ISO 10993-5.

A live/dead cytotoxicity assay was also performed to test the membrane integrity of the cells treated with sample eluents. In this method we used two

fluorescent components: Calcein AM (component A) and EthD-1 (component B). Calcein AM is a virtually nonfluorescent cell-permeant dye that converts to the intensely green fluorescent calcein in live cells by the presence of adequate esterase activity. Whereas, EthD-1 binds to the nucleic acid of dead cells, producing a bright red fluorescence. EthD-1 cannot enter live cells with the intact plasma membrane. Both components are virtually non-fluorescent before interacting with cells. Representative live/dead fluorescent microscopy images of the NIH 3T3 fibroblast cells that were incubated with samples extracts over the course of 72 h are shown in Figure 6. Cell morphology was normal at all time points and with respect to the total number of cells, very few dead (i.e., red) cells could be observed in all samples except the positive control latex that is known to be cytotoxic. Likewise, most cells stained green, indicating low level of toxicity from the samples extracts. MTT assay supported the live/dead data. PLA has been recognized by the FDA as appropriate for direct contact with biological fluids as early as the 1970's [5]. Comparing and contrasting the results obtained from both MTT and live/dead assays suggests the nontoxic nature of the extracts from CF_3-functionalized poly(lactic acid). It is important to acknowledge that this is an indirect and qualitative cytotoxicity evaluation. Further long-term and quantitative cytotoxicity studies are necessary to get a full picture of the cells

reaction to the polymer and its degradation products that may diffuse out of the polymer and into the surrounding culture media.

3.6. Protein adsorption

3.6.1. Protein adsorption from pure protein solutions

The adsorption of human serum Alb and Fg onto the polymer-coated coverslips and the 316 SS coupons from a pure Alb (0.3 mg/ml) and Fg (0.03 mg/ml) solution in cPBSzI is shown in Figures 7. The Alb and Fg concentrations were chosen to correspond to the concentration of these proteins in 1% human plasma [44, 45]. The protein adsorption results are compared with samples coated with poly(vinylidene fluoride-co-hexafluoropropylene) (PVDF-HFP) since this polymer have shown low thrombogenicity in clinical studies when used as a coating for XIENCE V® (Abbott Vascular) stents [46].

At the end of a 2 h adsorption time, both F-PLA and PVDF-HFP adsorbed relatively higher amounts of Alb than other samples. The Alb adsorption decreased in the order F-PLA and PVDF-HFP > PLA > 316 SS. After elution with 2% SDS, higher amounts of Alb were retained on both F-PLA and PVDF-HFP as compared to PLA and 316 SS. Statistically significant higher amount of albumin was adsorbed and retained on both F-PLA and PVDF-HFP as compared to all other materials studied ($\alpha = 0.05$). There was no statistically significant difference between the Alb adsorption and retention between F-PLA and PVDF-HFP.

Similar adsorption and retention trends were observed for pure Fg solution in cPBSzI with relatively greater amount of adsorbed and retained Fg on PVDF-HFP. The Fg adsorption decreased in the order of PVDF-HFP > F-PLA > PLA > 316 SS. Once again both F-PLA and PVDF-HFP retained relatively higher amount of Fg after elution with 2 % SDS.

3.6.2. Protein adsorption from binary/competitive protein solutions

The adsorption and retention of Alb and Fg onto the polymer coated coverslips and the 316 SS coupons from binary/competitive protein solutions is shown in Figure 8. To make these binary solutions, we prepared two identical 1% solutions containing both Alb and Fg in PBS based on the protein ratios observed in normal human blood plasma (Alb: 0.3 mg/ml to Fg: 0.03 mg/ml). Next, radiolabeled Alb was added to one solution and radiolabeled Fg to the other.

The Alb adsorption and retention trend in binary solutions was similar to the trend observed in pure protein solutions. Alb adsorption was in the range of 22-86 ng/cm^2 and once again F-PLA and PVDF-HFP both adsorbed and retained higher amounts of Alb as compared to PLA and 316 SS. Only negligible amounts of Alb (less than 3 ng/cm^2) were retained on PLA and 316 SS after elution with 2% SDS.

In the case of Fg, protein adsorption from an Alb-Fg binary protein solution was highest on PVDF-HFP (85 ng/cm^2) and F-PLA (83 ng/cm^2) and decreased in the order: PVDF-HFP > PLA-F > PLA > 316 SS. When both albumin and fibrinogen are present in the solution, samples overall adsorbed less Fg than from a pure Fg protein solution. The amount of the retained Fg after elution with 2% SDS was similar to the trend observed with retained Fg from pure protein solution. The highest amount of retained Fg was once again greater on PVDF-HFP (22 ng/cm^2) and F-PLA (20 ng/cm^2) and decreased in the same order as Fg adsorption.

In both cases, the amount of retained protein after elution with 2% SDS was statistically higher on F-PLA and PVDF-HFP than on all other samples tested here.

3.6.3. Protein adsorption from normal human plasma

Blood is complex fluid and contains more than 300 different proteins. To mimic the complex protein solutions that these surfaces might come into contact *in vivo*, we measured the protein adsorption onto these surfaces in 1% citrated pooled human plasma (Figure 9(a)). Human blood was drawn following the procedure described earlier and plasma was collected after removing blood cells by two step centrifugations and diluted to 1 % plasma by adding cPBSz buffer.

Overall, the amount of adsorbed Alb and Fg from human plasma was noticeably lower than that measured in pure and binary protein solutions. All samples had higher Alb adsorption than Fg except 316 SS. In addition, F-PLA and PVDF-HFP both adsorbed statistically higher amount of Alb as compared to PLA and 316 SS. Figure 9(b) Shows the protein retention after elution with 2% SDS. Once again, a statistically higher amount of both Alb and Fg were retained on the PVDF-HFP (Alb: 13 ng/cm^2, Fg: 14 ng/cm^2) and F-PLA (Alb: 11 ng/cm^2, Fg: 10 ng/cm^2) as compared to PLA and 316 SS. Of all the samples, 316 SS retained the least adsorbed protein with marginally higher amounts of Alb than Fg.

The Alb/Fg ratio of the adsorbed and retained proteins from 1% human plasma is shown in Table I. The Alb/Fg protein adsorption ratios (mass basis) ranged from 1.7 to 0.8, with the highest value for F-PLA. Upon elution with 2 % SDS, the Alb/Fg ratio was changed for all the surfaces and ranged from 1.44 to 0.92.

Protein adsorption from blood plasma provides a more realistic assessment of the relative affinity of surfaces for a specific protein competing with other proteins in the complex mixture of human plasma. When protein adsorption was measured from pure, binary and 1% plasma protein solutions, PLA and 316 SS had the lowest adsorbed and retained Alb and Fg. On the other hand, F-PLA and PVDF-HFP had the highest protein adsorption and retention after incubating with 2% SDS.

Our observations of protein adsorption and retention on fluorinated surfaces is consistent with the previous studies which reported higher retention of proteins on fluorinated surfaces [47, 48]. Fluorinated materials have been approved for use in various blood-contacting applications due to their satisfactory clinical performance [49-51].

Although there are no universally-accepted guidelines for blood compatibility evaluation of synthetic materials, studies are generally focused on blood plasma protein adsorption, platelet interaction and activation of the intrinsic pathway [52-56]. Protein adsorption at biomaterial surfaces is considered a key, initial event after implantation and is thought to be central to the ultimate outcome. Protein adsorption is dependent on the physiochemical properties of both proteins and surfaces. Upon contact, proteins from plasma can be adsorbed to the biomaterial surface in seconds and form a 2-10 nm monolayer, resulting a high concentration of the proteins at the interface as compared to their concentrations in plasma [45, 57, 58].

The current research is focused on the interaction of two blood plasma proteins, albumin and fibrinogen, with the fluoropolymer surfaces. Albumin is the most abundant blood protein (concentration: 35-50 mg/ml) and has high affinity for circulating free fatty acids. It has been shown that highly hydrophobic surfaces can develop a strong interaction with albumin and retain it on their surfaces.

Studies by Leclercq *et al.* [59, 60] showed that surfaces with a layer of adsorbed albumin reduced the adsorption of other proteins (mixture of albumin, fibrinogen and γ-globulins at physiological concentrations) when they were presented individually and when they were mixed. In addition, the albumin coating minimized the adsorption of other proteins, specially fibrinogen, when the three proteins presented sequentially. This is considered a potentially thromboresistant effect since a preadsorbed layer of albumin has minimal interaction with blood platelets and might also inhibit the subsequent adsorption of fibrinogen and other proteins [61, 62]. Fg (concentration: 2-4.5 mg/ml) has been shown to play a key role in initiating coagulation and adsorbed Fg, even at low levels, can trigger platelet adhesion and activation [63-66]. However, adsorption to some surfaces renders the Fg relatively inactive to platelets [66, 67]. Thus, generalizations about the importance of Fg to blood compatibility are not simple to make.

Two mechanisms have been proposed to explain the passivation effect of the adsorbed albumin layer: (1) blockage of surface active sites preventing the surface contact-initiating step, and (2) complexing of the surface-bound albumin with surface contact-activated plasma proteins [61]. We have modified this hypothesis and introduced an Alb/Fg ratio to include the fibrinogen adsorption in competition with albumin. Earlier studies suggest that a high Alb/Fg ratio

contributes to improved hemocompatibility of polymer surfaces [68]. Also, high albumin retention, sometimes referred to as "albumin tight binding" should be taken into consideration for a more mechanistic view of the events at the blood-biomaterial interface. This is particularly important since protein adsorption from blood plasma involves a complex series of adsorption and displacement steps known as "Vroman effect". This competitive protein exchange is a general phenomenon and occurs when a protein mixture adsorbs to a surface and then early adsorbers are subsequently displaced by high affinity binding proteins that are present in the solution. The high retention of albumin on some fluorinated surfaces suggests these surfaces may resist the displacement of albumin by fibrinogen [69, 70] leading to enhanced, long-term blood compatibility.

4. Conclusions

We have developed a novel synthetic method for preparing CF_3-functionalized poly(lactic acid). First, we synthesized the CF_3-functionalized monomer and then optimized the ROP to prepare the subsequent polymer. As expected the resulted polymer showed higher hydrophobicity relative to unmodified PLA. There was no observed cytotoxicity from materials extracts as confirmed by both MTT and live/dead staining methods on NIH-3T3 mouse fibroblast cells.

This approach can potentially extend the scope of physiochemical properties and biomedical applications of polylactides. Further optimization of the synthetic reaction and the development of effective purification/fractionation techniques of the polymerization reagents will enable us to obtain higher molecular weight polymers. In addition, ongoing studies are aimed at investigating the degradation characteristics and by-product of this degradation in more details. Both PVDF-HFP and CF_3-functionalized poly(lactic acid) have demonstrated adsorption and retention (after incubation with 2% SDS) of higher amount of the albumin and fibrinogen in single and binary protein solutions and plasma. Along with a higher Alb/Fg ratio, we hypothesize that these fluoropolymers will demonstrate enhanced thromboresistance *in vivo*. Additional investigations will be carried out to address the blood compatibility of this new class of degradable polyesters by analyzing platelet interactions and activation of the intrinsic clotting system under flow conditions.

Acknowledgements

This work was supported by Abbott Vascular, Inc. and Center for Dialysis Innovation (CDI) at the University of Washington. Part of this work was conducted at the Molecular Analysis Facility, a National Nanotechnology Coordinated Infrastructure site at the University of Washington which is supported in part by the National Science Foundation (grant ECC-1542101), the

University of Washington, the Molecular Engineering & Sciences Institute, the Clean Energy Institute, and the National Institutes of Health. We also would like to thank Prof. Christine Luscombe, Prof. Andrew Boydston, Dr. Raj Paranji, Dr. Jean Rene-Ella-Menye, Dr. Anna Galperin, Dr. Chang-uk Lee and Prof. Esmaeel Naeemi (Seattle Central Community College) for his experimental assistance on synthesis and characterizations of monomer and polymer and Prof. Thomas Horbett (University of Washington), for his insightful comments related to protein adsorptions studies. We thank Dr. Kyle Caldwell and Prof. John C. Berg (University of Washington) for technical discussions and experimental assistance on contact angle measurements.

Reference:

[1] P. Saini, M. Arora, M. Kumar, Poly(lactic acid) blends in biomedical applications, Adv Drug Deliv Rev 107 (2016) 47-59.

[2] Y. Ramot, M. Haim-Zada, A.J. Domb, A. Nyska, Biocompatibility and safety of PLA and its copolymers, Adv Drug Deliv Rev 107 (2016) 153-162.

[3] S. Farah, D.G. Anderson, R. Langer, Physical and mechanical properties of PLA, and their functions in widespread applications - A comprehensive review, Adv Drug Deliv Rev 107 (2016) 367-392.

[4] P.W.J.C. Serruys, Y. Onuma, Bioresorbable Scaffolds: From Basic Concept to Clinical Applications, Boca Raton, FL, 2017.

[5] R.M. Rasal, A.V. Janorkar, D.E. Hirt, Poly(lactic acid) modifications, Progress in Polymer Science 35(3) (2010) 338-356.

[6] C. Regnier-Delplace, O. Thillaye du Boullay, F. Siepmann, B. Martin-Vaca, P. Demonchaux, O. Jentzer, F. Danede, M. Descamps, J. Siepmann, D. Bourissou, PLGAs bearing carboxylated side chains: novel matrix formers with improved properties for controlled drug delivery, J Control Release 166(3) (2013) 256-67.

[7] Y. Yu, J. Zou, C. Cheng, Synthesis and biomedical applications of functional poly(α-hydroxyl acid)s, Polymer Chemistry 5(20) (2014) 5854-5872.

[8] M. Yin, G.L. Baker, Preparation and Characterization of Substituted Polylactides, Macromolecules 32(23) (1999) 7711-7718.

[9] T. Trimaille, M. Möller, R. Gurny, Synthesis and ring-opening polymerization of new monoalkyl-substituted lactides, Journal of Polymer Science Part A: Polymer Chemistry 42(17) (2004) 4379-4391.

[10] T. Liu, T.L. Simmons, D.A. Bohnsack, M.E. Mackay, M.R. Smith, G.L. Baker, Synthesis of Polymandelide: A Degradable Polylactide Derivative with Polystyrene-like Properties, Macromolecules 40(17) (2007) 6040-6047.

[11] M. Leemhuis, C.F. van Nostrum, J.A.W. Kruijtzer, Z.Y. Zhong, M.R. ten Breteler, P.J. Dijkstra, J. Feijen, W.E. Hennink, Functionalized Poly(α-hydroxy acid)s via Ring-Opening Polymerization: Toward Hydrophilic Polyesters with Pendant Hydroxyl Groups, Macromolecules 39(10) (2006) 3500-3508.

[12] W.W. Gerhardt, D.E. Noga, K.I. Hardcastle, A.J. Garcia, D.M. Collard, M. Weck, Functional lactide monomers: methodology and polymerization, Biomacromolecules 7(6) (2006) 1735-42.

[13] X. Jiang, E.B. Vogel, M.R. Smith Iii, G.L. Baker, Amphiphilic PEG/alkyl-grafted comb polylactides, Journal of Polymer Science Part A: Polymer Chemistry 45(22) (2007) 5227-5236.

[14] D.B. McKie, S. Lepeniotis, Optimization techniques for carbodiimide activated synthesis of poly((RS)-3,3,3-trifluorolactic acid); statistically designed experiments to optimize polymerization conditions, Chemometrics and Intelligent Laboratory Systems 41(1) (1998) 105-113.

[15] C.-U. Lee, R. Khalifehzadeh, B. Ratner, A.J. Boydston, Facile Synthesis of Fluorine-Substituted Polylactides and Their Amphiphilic Block Copolymers, Macromolecules 51(4) (2018) 1280-1289.

[16] K. Muller, C. Faeh, F. Diederich, Fluorine in pharmaceuticals: looking beyond intuition, Science 317(5846) (2007) 1881-6.

[17] Y. Yamamoto, T. Kurohara, M. Shibuya, CF3-Substituted semisquarate: a pluripotent building block for the divergent synthesis of trifluoromethylated functional molecules, Chem Commun (Camb) 51(91) (2015) 16357-60.

[18] P.A. Champagne, J. Desroches, J.D. Hamel, M. Vandamme, J.F. Paquin, Monofluorination of Organic Compounds: 10 Years of Innovation, Chem Rev 115(17) (2015) 9073-174.

[19] J. Wang, M. Sanchez-Rosello, J.L. Acena, C. del Pozo, A.E. Sorochinsky, S. Fustero, V.A. Soloshonok, H. Liu, Fluorine in pharmaceutical industry: fluorine-containing drugs introduced to the market in the last decade (2001-2011), Chem Rev 114(4) (2014) 2432-506.

[20] K.L. Kirk, Fluorination in Medicinal Chemistry: Methods, Strategies, and Recent Developments, Organic Process Research & Development 12(2) (2008) 305-321.

[21] R.Y. Kannan, H.J. Salacinski, P.E. Butler, G. Hamilton, A.M. Seifalian, Current status of prosthetic bypass grafts: a review, J Biomed Mater Res B Appl Biomater 74(1) (2005) 570-81.

[22] A.I. Cassady, N.M. Hidzir, L. Grøndahl, Enhancing expanded poly(tetrafluoroethylene) (ePTFE) for biomaterials applications, Journal of Applied Polymer Science 131(15) (2014).

[23] J.G. Riess, M.P. Krafft, Fluorinated materials for *in vivo* oxygen transport (blood substitutes), diagnosis and drug delivery, Biomaterials 19(16) (1998) 1529-39.

[24] C.C. Tsai, H.H. Huo, P. Kulkarni, R.C. Eberhart, Biocompatible coatings with high albumin affinity, ASAIO Trans 36(3) (1990) M307-10.

[25] R. Khalifehzadeh, W. Ciridon, B.D. Ratner, Surface fluorination of polylactide as a path to improve platelet associated hemocompatibility, Acta Biomater 78 (2018) 23-35.

[26] C.Y. Tham, Z.A.A. Hamid, Z.A. Ahmad, H. Ismail, Surface Engineered Poly(lactic acid) (PLA) Microspheres by Chemical Treatment for Drug Delivery System, Key Engineering Materials 594-595 (2014) 214-218.

[27] M.A. Elsawy, K.-H. Kim, J.-W. Park, A. Deep, Hydrolytic degradation of polylactic acid (PLA) and its composites, Renewable and Sustainable Energy Reviews 79 (2017) 1346-1352.

[28] U. Schöllkopf, W. Hartwig, U. Sprotte, W. Jung, Lactidkontraktion, eine Methode zur Synthese von α, α'- Dihydroxyketonen aus α-Hydroxycarbonsäuren, Angewandte Chemie 91(4) (1979) 329-330.

[29] Q. Zhang, H. Ren, G.L. Baker, Synthesis and click chemistry of a new class of biodegradable polylactide towards tunable thermo-responsive biomaterials, Polym Chem 6(8) (2015) 1275-1285.

[30] J.L. Brash, P. ten Hove, Effect of plasma dilution on adsorption of fibrinogen to solid surfaces, Thromb Haemost 51(3) (1984) 326-30.

[31] R. Nagase, Y. Iida, M. Sugi, T. Misaki, Y. Tanabe, Improved Robust Method for Preparing Optically Active 3-Alkyl-3-Phenyl-1,4-Dioxane-2,5-diones, a New Promising Chiral Template, Synthesis 22 (2008) 3670-3674.

[32] Q. Yin, L. Yin, H. Wang, J. Cheng, Synthesis and biomedical applications of functional poly(alpha-hydroxy acids) via ring-opening polymerization of O-carboxyanhydrides, Acc Chem Res 48(7) (2015) 1777-87.

[33] Y. Hu, W.A. Daoud, K.K.L. Cheuk, C.S.K. Lin, Newly Developed Techniques on Polycondensation, Ring-Opening Polymerization and Polymer Modification: Focus on Poly(Lactic Acid), Materials (Basel) 9(3) (2016).

[34] O. Dechy-Cabaret, B. Martin-Vaca, D. Bourissou, Controlled ring-opening polymerization of lactide and glycolide, Chem Rev 104(12) (2004) 6147-76.

[35] S. Kaihara, S. Matsumura, A.G. Mikos, J.P. Fisher, Synthesis of poly(L-lactide) and polyglycolide by ring-opening polymerization, Nat Protoc 2(11) (2007) 2767-71.

[36] S.H. Hyon, K. Jamshidi, Y. Ikada, Synthesis of polylactides with different molecular weights, Biomaterials 18(22) (1997) 1503-8.

[37] S. Dutta, W.-C. Hung, B.-H. Huang, C.-C. Lin, Recent Developments in Metal-Catalyzed Ring-Opening Polymerization of Lactides and Glycolides: Preparation of Polylactides, Polyglycolide, and Poly(lactide-co-glycolide), in: B. Rieger, A. Künkel, G.W. Coates, R. Reichardt, E. Dinjus, T.A. Zevaco (Eds.), Synthetic Biodegradable Polymers, Springer Berlin Heidelberg, Berlin, Heidelberg, 2012, pp. 219-283.

[38] S. Slomkowski, S. Penczek, A. Duda, Polylactides—an overview, Polymers for Advanced Technologies 25(5) (2014) 436-447.

[39] D. Han, L. Zhu, Y. Chen, W. Li, X. Wang, L. Ning, Synthesis of fluorinated monomer and formation of hydrophobic surface therefrom, RSC Advances 5(29) (2015) 22847-22855.

[40] W. Ming, J. Laven, R. van der Linde, Synthesis and Surface Properties of Films Based on Solventless Liquid Fluorinated Oligoester, Macromolecules 33(18) (2000) 6886-6891.

[41] H. Tavana, F. Simon, K. Grundke, D.Y. Kwok, M.L. Hair, A.W. Neumann, Interpretation of contact angle measurements on two different fluoropolymers for the determination of solid surface tension, J Colloid Interface Sci 291(2) (2005) 497-506.

[42] H. Tavana, D. Jehnichen, K. Grundke, M.L. Hair, A.W. Neumann, Contact angle hysteresis on fluoropolymer surfaces, Adv Colloid Interface Sci 134-135 (2007) 236-48.

[43] D.F. Cheng, B. Masheder, C. Urata, A. Hozumi, Smooth Perfluorinated Surfaces with Different Chemical and Physical Natures: Their Unusual Dynamic Dewetting Behavior toward Polar and Nonpolar Liquids, Langmuir 29(36) (2013) 11322-11329.

[44] N.L. Anderson, N.G. Anderson, The human plasma proteome: history, character, and diagnostic prospects, Mol Cell Proteomics 1(11) (2002) 845-67.

[45] I.H. Jaffer, J.C. Fredenburgh, J. Hirsh, J.I. Weitz, Medical device-induced thrombosis: what causes it and how can we prevent it?, Journal of Thrombosis and Haemostasis 13(S1) (2015) S72-S81.

[46] E. Grube, B. Chevalier, P. Smits, V. Dzavik, T.M. Patel, A.S. Mullasari, J. Wohrle, M. Stuteville, C. Dorange, U. Kaul, S.V. Investigators, The SPIRIT V study: a clinical evaluation of the XIENCE V everolimus-eluting coronary stent system in the treatment of patients with de novo coronary artery lesions, JACC Cardiovasc Interv 4(2) (2011) 168-75.

[47] J.L. Bohnert, B.C. Fowler, T.A. Horbett, A.S. Hoffman, Plasma gas discharge deposited fluorocarbon polymers exhibit reduced elutability of adsorbed albumin and fibrinogen, J Biomater Sci Polym Ed 1(4) (1990) 279-97.

[48] L.M. Szott, C.A. Irvin, M. Trollsas, S. Hossainy, B.D. Ratner, Blood compatibility assessment of polymers used in drug eluting stent coatings, Biointerphases 11(2) (2016) 029806-029806.

[49] J.P. Eiberg, O. Roder, M. Stahl-Madsen, N. Eldrup, P. Qvarfordt, A. Laursen, M. Greve, T. Florenes, O.M. Nielsen, C. Seidelin, T. Vestergaard-Andersen, T.V. Schroeder, Fluoropolymer-coated dacron versus PTFE grafts for femorofemoral crossover bypass: randomised trial, Eur J Vasc Endovasc Surg 32(4) (2006) 431-8.

[50] L. Pedrini, M. Dondi, A. Magagnoli, F. Magnoni, E. Pisano, E. Del Giudice, M. Santoro, Evaluation of thrombogenicity of fluoropassivated polyester patches following carotid endarterectomy, Ann Vasc Surg 15(6) (2001) 679-83.

[51] G. Laroche, Y. Marois, R. Guidoin, M.W. King, L. Martin, T. How, Y. Douville, Polyvinylidene fluoride (PVDF) as a biomaterial: From polymeric raw material to monofilament vascular suture, Journal of Biomedical Materials Research 29(12) (1995) 1525-1536.

[52] B.D. Ratner, The catastrophe revisited: blood compatibility in the 21st Century, Biomaterials 28(34) (2007) 5144-7.

[53] I. Reviakine, S. Braune, Preface: In Focus Issue on Blood-Biomaterial Interactions, Biointerphases 11(2) (2016) 029501.

[54] S.L. Blok, G.E. Engels, W. van Oeveren, *In vitro* hemocompatibility testing: The importance of fresh blood, Biointerphases 11(2) (2016) 029802.

[55] M.B. Gorbet, M.V. Sefton, Biomaterial-associated thrombosis: roles of coagulation factors, complement, platelets and leukocytes, Biomaterials 25(26) (2004) 5681-703.

[56] I. Reviakine, F. Jung, S. Braune, J.L. Brash, R. Latour, M. Gorbet, W. van Oeveren, Stirred, shaken, or stagnant: What goes on at the blood–biomaterial interface, Blood Reviews 31(1) (2017) 11-21.

[57] Y. Wu, F.I. Simonovsky, B.D. Ratner, T.A. Horbett, The role of adsorbed fibrinogen in platelet adhesion to polyurethane surfaces: a comparison of surface hydrophobicity, protein adsorption, monoclonal antibody binding, and platelet adhesion, J Biomed Mater Res A 74(4) (2005) 722-38.

[58] C.J. Wilson, R.E. Clegg, D.I. Leavesley, M.J. Pearcy, Mediation of biomaterial-cell interactions by adsorbed proteins: a review, Tissue Eng 11(1-2) (2005) 1-18.

[59] L. Leclercq, M. Vert, Comparison between protein repulsions by diblock PLA-PEO and albumin nanocoatings using OWLS, J Biomater Sci Polym Ed 28(2) (2017) 177-193.

[60] L. Leclercq, E. Modena, M. Vert, Adsorption of proteins at physiological concentrations on pegylated surfaces and the compatibilizing role of adsorbed albumin with respect to other proteins according to optical waveguide lightmode spectroscopy (OWLS), J Biomater Sci Polym Ed 24(13) (2013) 1499-518.

[61] R.C. Eberhart, M.S. Munro, J.R. Frautschi, M. Lubin, F.J. Clubb, Jr., C.W. Miller, V.I. Sevastianov, Influence of endogenous albumin binding on blood-material interactions, Ann N Y Acad Sci 516 (1987) 78-95.

[62] K. Kottke-Marchant, J.M. Anderson, Y. Umemura, R.E. Marchant, Effect of albumin coating on the *in vitro* blood compatibility of Dacron arterial prostheses, Biomaterials 10(3) (1989) 147-55.

[63] J.M. Grunkemeier, W.B. Tsai, C.D. McFarland, T.A. Horbett, The effect of adsorbed fibrinogen, fibronectin, von Willebrand factor and vitronectin on the procoagulant state of adherent platelets, Biomaterials 21(22) (2000) 2243-52.

[64] W.B. Tsai, Q. Shi, J.M. Grunkemeier, C. McFarland, T.A. Horbett, Platelet adhesion to radiofrequency glow-discharge-deposited fluorocarbon polymers preadsorbed with selectively depleted plasmas show the primary role of fibrinogen, J Biomater Sci Polym Ed 15(7) (2004) 817-40.

[65] B. Sivaraman, R.A. Latour, The adherence of platelets to adsorbed albumin by receptor-mediated recognition of binding sites exposed by adsorption-induced unfolding, Biomaterials 31(6) (2010) 1036-44.

[66] A. Chiumiento, S. Lamponi, R. Barbucci, Role of fibrinogen conformation in platelet activation, Biomacromolecules 8(2) (2007) 523-31.

[67] W.B. Tsai, J.M. Grunkemeier, T.A. Horbett, Variations in the ability of adsorbed fibrinogen to mediate platelet adhesion to polystyrene-based materials: a multivariate statistical analysis of antibody binding to the platelet binding sites of fibrinogen, J Biomed Mater Res A 67(4) (2003) 1255-68.

[68] D.J. Lyman, L.C. Metcalf, D. Albo, Jr., K.F. Richards, J. Lamb, The effect of chemical structure and surface properties of synthetic polymers on the coagulation of blood. III. *In vivo* adsorption of proteins on polymer surfaces, Trans Am Soc Artif Intern Organs 20 B (1974) 474-8.

[69] S.Y. Jung, S.M. Lim, F. Albertorio, G. Kim, M.C. Gurau, R.D. Yang, M.A. Holden, P.S. Cremer, The Vroman effect: a molecular level description of fibrinogen displacement, J Am Chem Soc 125(42) (2003) 12782-6.

[70] S.L. Hirsh, D.R. McKenzie, N.J. Nosworthy, J.A. Denman, O.U. Sezerman, M.M. Bilek, The Vroman effect: competitive protein exchange with dynamic multilayer protein aggregates, Colloids Surf B Biointerfaces 103 (2013) 395-404.

Figures

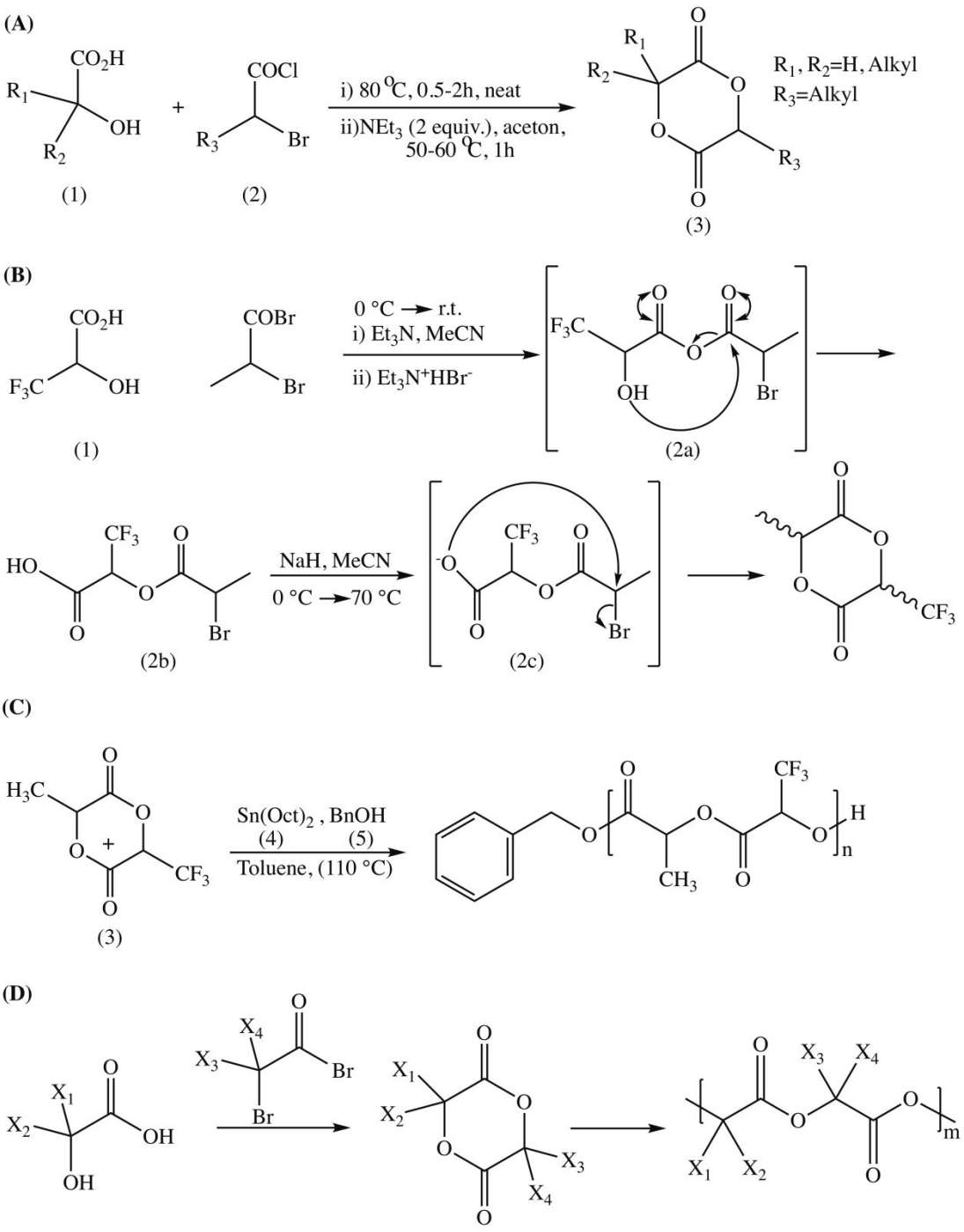

Figure 1. Synthetic routes and reaction pathways described in this work. (A) Synthesis of alkyl-substituted lactide by Schollkopf's method. (B) Preparation of trifluoromethyl-functionalized lactide monomer and proposed cyclocondensation mechanism. (C) Ring-opening polymerization of trifluoromethyl-functionalized poly(lactic acid) and polymerization conditions. (D) General synthesis approach of halogen-substituted lactide monomer and subsequent halogenated polymer. At least one of x_1 or x_2 is halogen or

halocarbon.

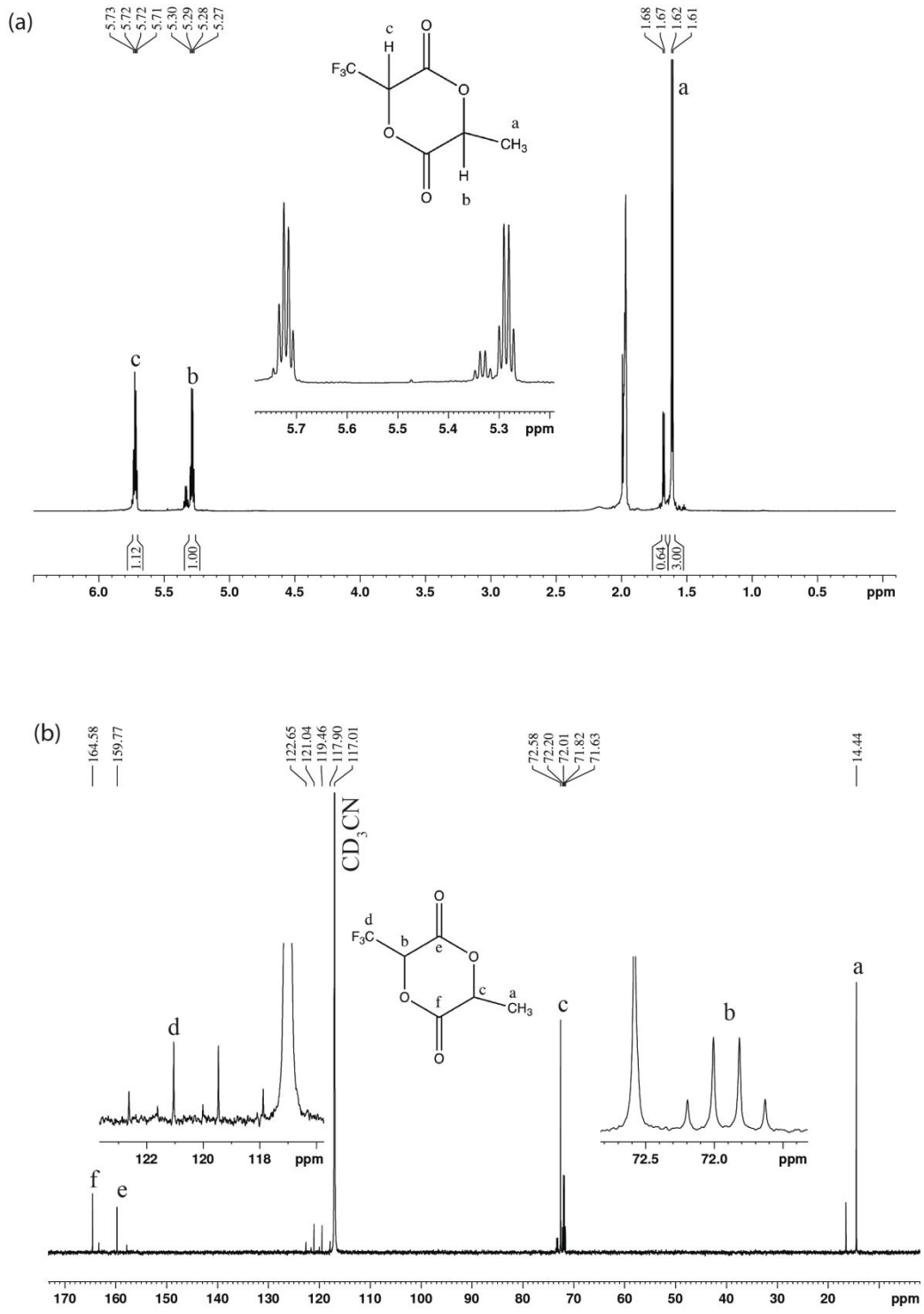

Figure 2. (a) ^{1}H-NMR and (b) ^{13}C-NMR spectrum (700 MHz, CD_3CN) of

trifluoromethyl-functionalized lactide monomer.

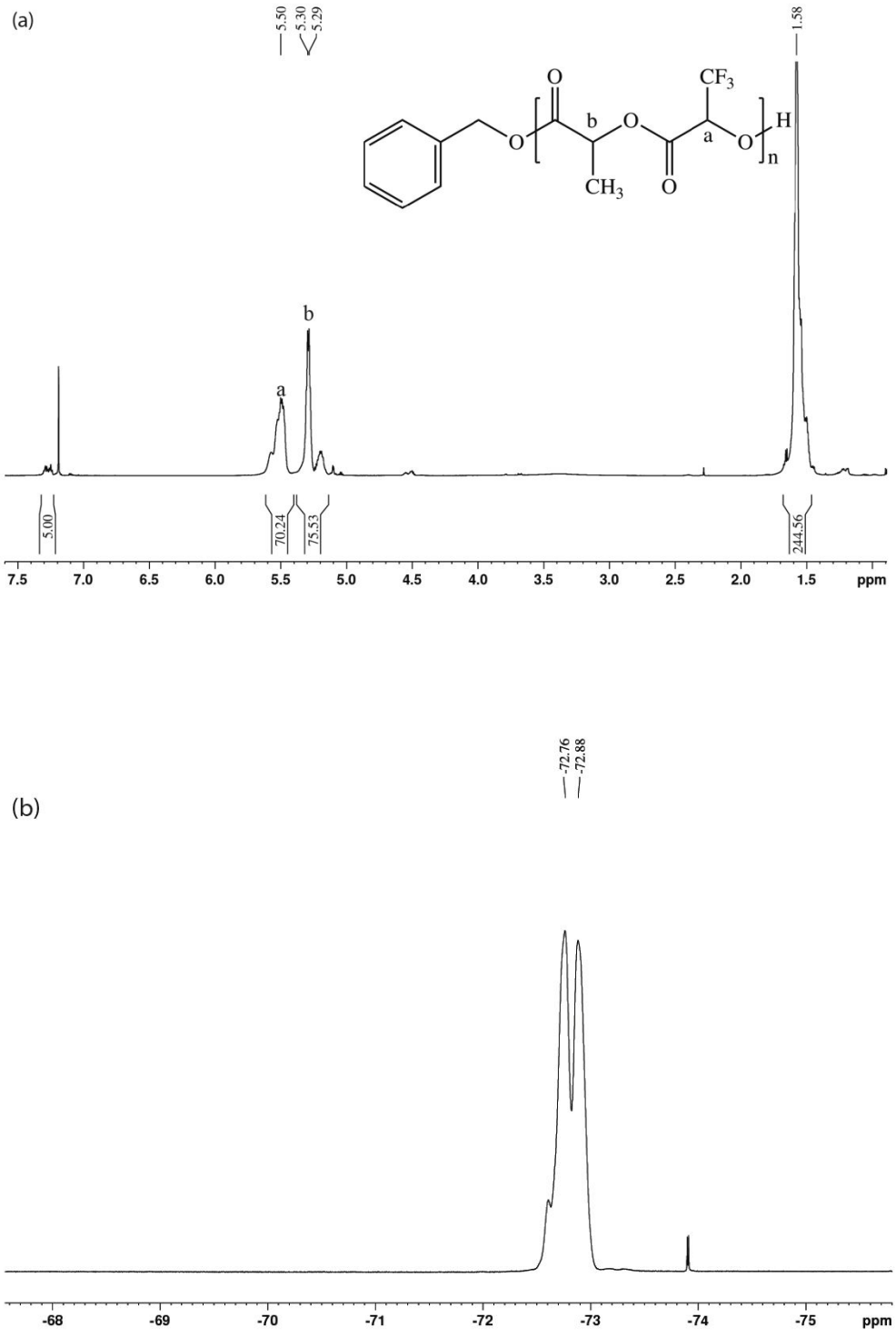

Figure 3. (a) ^{1}H-NMR spectrum (700 MHz, $CDCl_3$) and (b) ^{19}F-NMR spectrum

(500 MHz, $CDCl_3$) with ^1H decoupling of trifluoromethyl-functionalized poly(lactic acid).

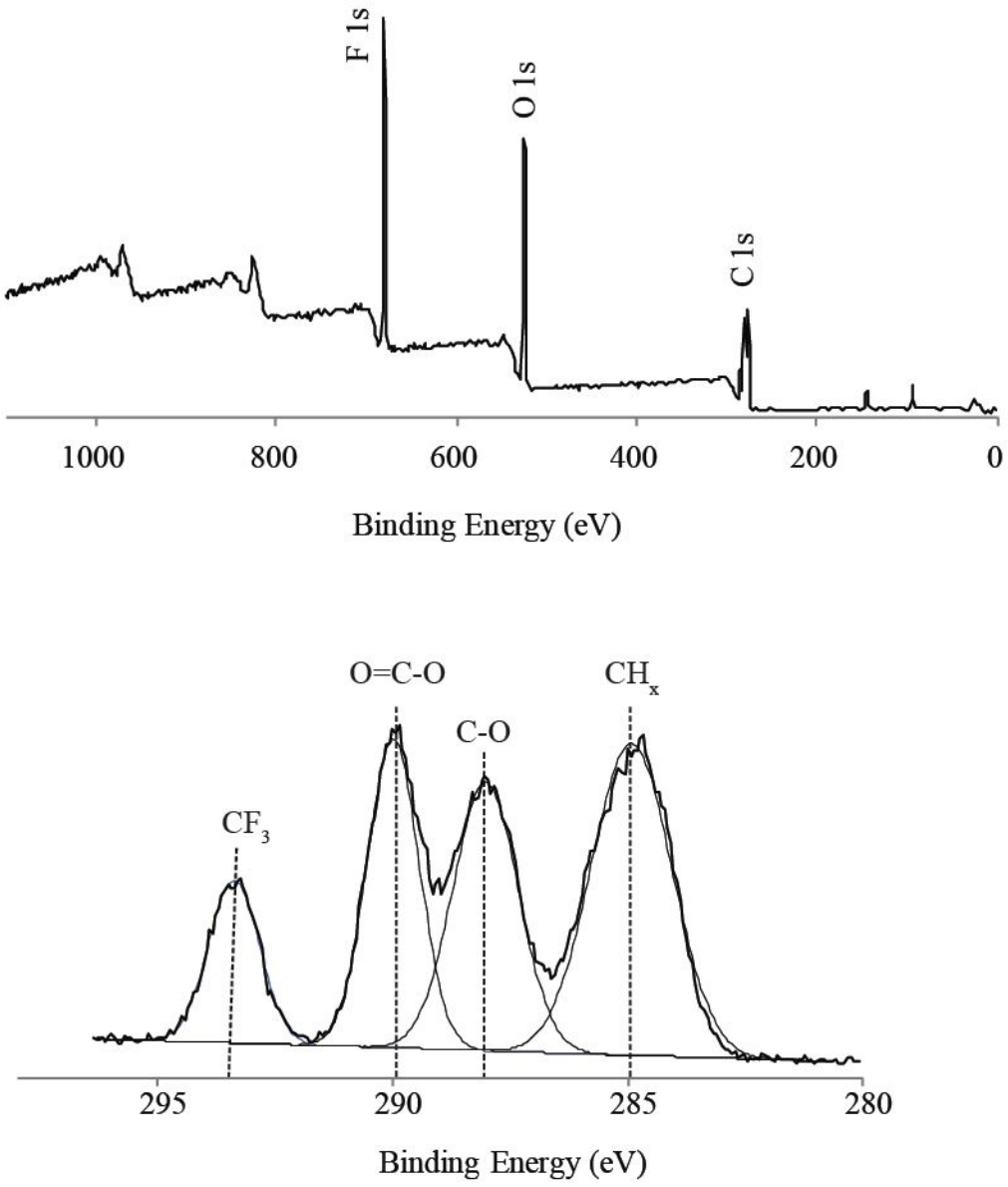

Figure 4. ESCA spectrum of trifluoromethyl-functionalized poly(lactic acid) (top) and its high-resolution C1s spectrum and curve fitting (bottom). From left to right, the peaks correspond to CF_3, O=C–O, C–O, and CH_3. In addition to C1s and O1s peaks, we observed an F1s peak in the ESCA spectrum.

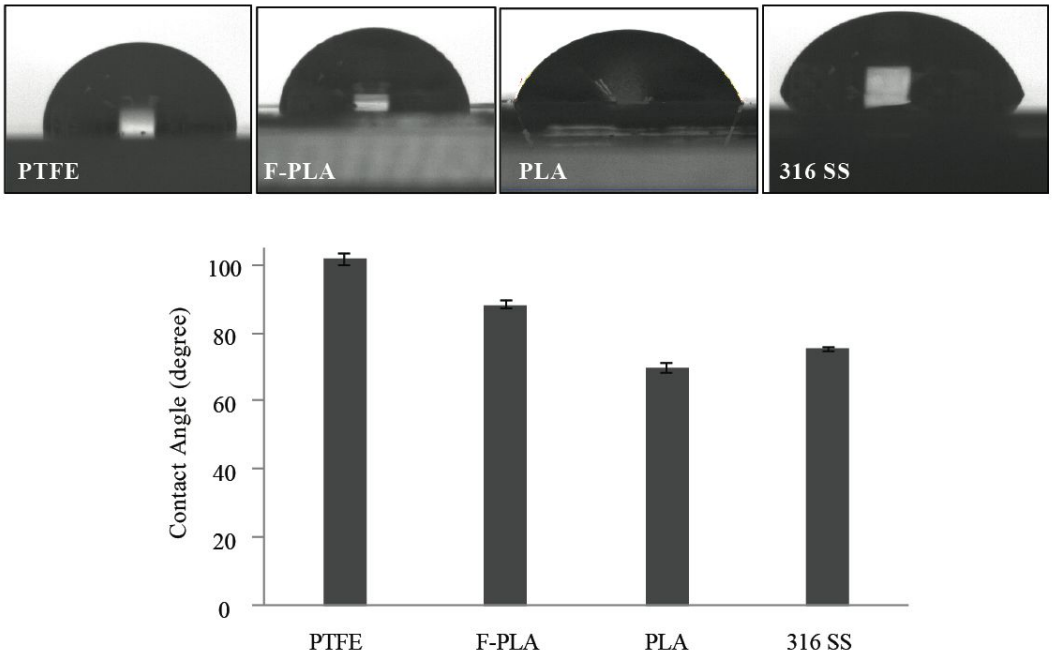

Figure 5. The profiles of water droplets on the surface of trifluoromethyl-functionalized poly(lactic acid) (F-PLA) measured by aqueous sessile drop goniometry and its comparison with PTFE, PLA and stainless steel.

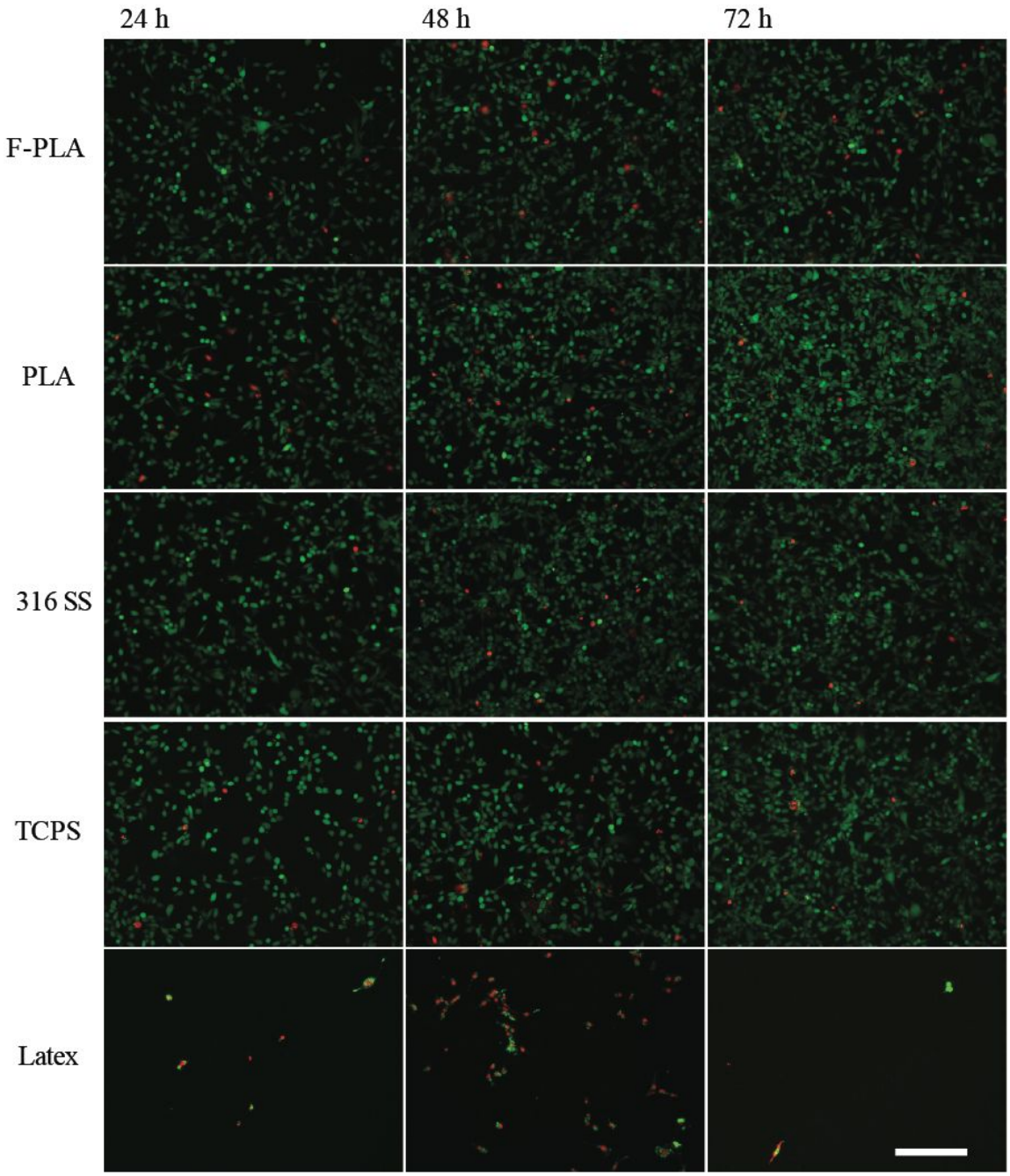

Figure 6. Live/dead staining of NIH-3T3 cells treated with trifluoromethyl-functionalized poly(lactic acid) extracts and its comparison with positive (latex) and negative (TCPS) controls. Calcein is staining live cells (green), and propidium iodide is staining dead cells (red). Over the course of 72 h incubation with sample extracts, the majority of cells stained green in all the samples tested here except the positive control. (Scale bar: 400 μm).

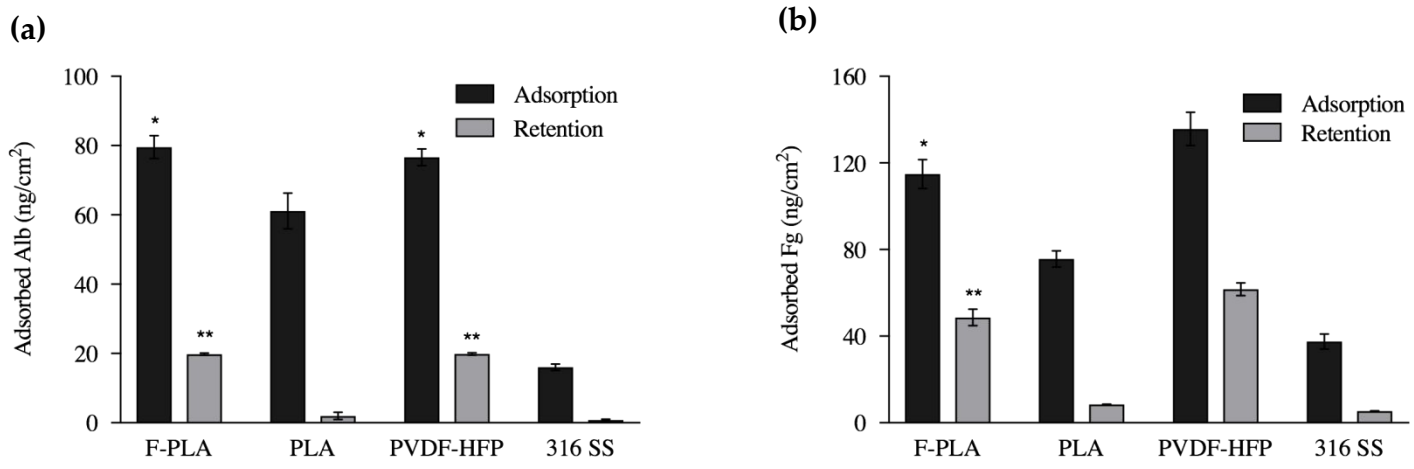

Figure 7. (a) Protein adsorption from a pure Alb solution (0.3 mg/ml) in cPBSzI and the retained Alb on the surfaces after 24 h elution with 2% SDS. Single asterisk (*) shows statistically significant higher amount of adsorbed Alb on both F-PLA and PVDF-HFP as compared to PLA and 316 SS. Double asterisk (**) shows statistically significant higher amount of retained Alb on both F-PLA and PVDF-HFP as compared to all other materials tested ($\alpha \leq 0.05$). There was no statistically significant difference in Alb adsorption and retention between F-PLA and PVDF-HFP. (b) Protein adsorption from a pure Fg solution (0.03 mg/ml) in cPBSzI and the retained Fg on the surfaces after 24 h elution with 2% SDS (right)Single asterisk (*) and double asterisk (**) show statistically significant difference between the amount of adsorbed and retained Fg on F-PLA as compared to all other materials tested here ($\alpha \leq 0.05$). Error bars indicate SEM, n=6.

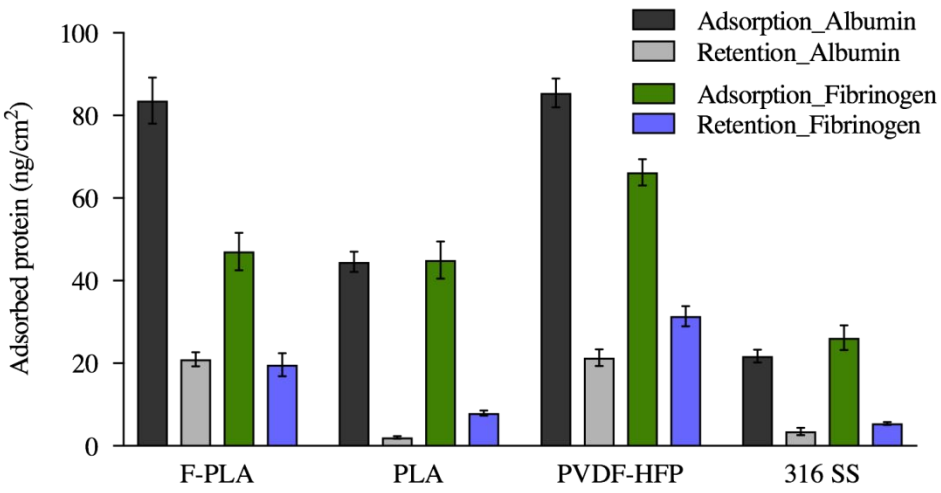

Figure 8. Competitive protein adsorption from binary solutions (Alb: 0.3 mg/ml and Fg: 0.03mg/ml). Samples were incubated for 2 h in binary protein solutions in cPBSZI (black and gray). The amount of retained protein on the surfaces was measured after 24 h incubation with 2% SDS (green and blue). There is a statistically significant greater amount of both adsorbed and retained Alb on F-PLA and PVDF-HFP as compared to other samples. There is a significantly higher amount of retained Fg on both F-PLA and PVDF-HFP as compared to PLA and 316 SS ($\alpha \leq 0.05$). Error bars indicate SEM, n=6.

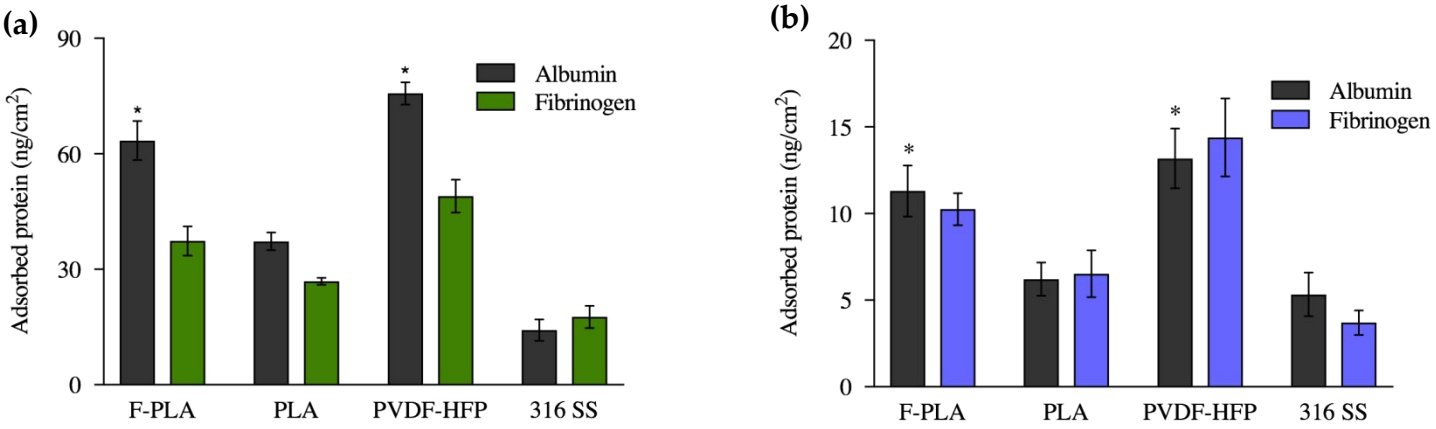

Figure 9. (a) Protein adsorption from 1 % citrated normal human plasma. Black bars represent Alb adsorption and green bars show Fg adsorption. Single asterisk (*) shows statistically significant higher amount of adsorbed Alb on both F-PLA and PVDF-HFP as compared to all other samples ($\alpha \leq 0.05$). (b)

Protein retention from 1 % citrated normal human plasma after 24 h elution with 2% SDS. Retained Alb is shown in black and retained Fg is shown in blue. Single asterisk (*) shows statistically significant higher amount of retained Alb on both F-PLA and PVDF-HFP as compared to PLA and 316 SS ($\alpha \leq 0.05$). Error bars indicate SEM, n=6.

Table 1. Alb/Fg ratio (mass basis) of different samples after 2 h adsorption in 1 % citrated normal human plasma and subsequent elution with 2% SDS for 24 h.

Sample	Alb/Fg Adsorption	Alb/Fg Retention
F-PLA	1.70	1.10
PLA	1.39	0.95
PVDF-HFP	1.55	0.92
316 SS	0.80	1.44

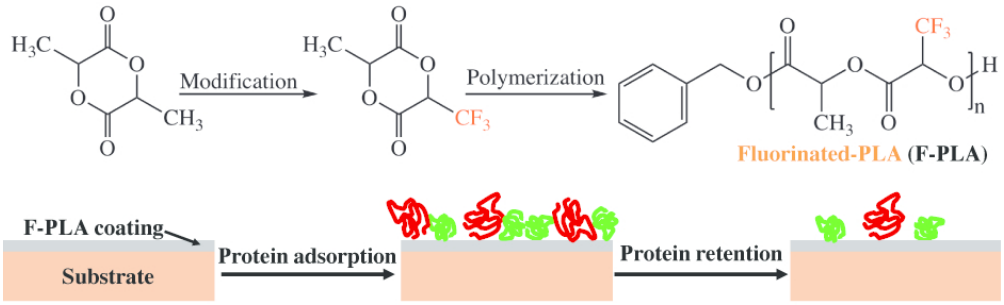
Modification
Polymerization
Fluorinated-PLA (F-PLA)
F-PLA coating
Substrate
Protein adsorption
Protein retention